

# Syntheses of Cyclic Poly(L-lactide)s by Means of Zinc-Based Ring-Opening Polymerization with Simultaneous Polycondensation (ROPPOC) Catalysts

Hans R. Kricheldorf,\* Felix Scheliga, and Steffen M. Weidner

Ring-opening polymerizations of L-lactide are studied in bulk at 140 or 160 °C with zinc *n*-hexanoate, zinc 4-chlorothiophenolate, and zinc pentafluoro thiophenolate (ZnSPF) as catalysts. The reactivity increases in the given order. With all three catalysts a high fraction of cycles is obtained only at polymerization (annealing) times around 7 d. With ZnSPF weight average molecular weights ( $M_w$ ) up to 178 000, a  $T_m$  around 199 °C and a  $\Delta H_m$  around 99 J g<sup>-1</sup> were achieved. The samples annealed for 4 or 7 d also display a saw tooth pattern of the mass peak distribution in the matrix-assisted laser desorption/ionization time of flight spectra indicating transesterification reactions across the surface of extended ring crystals. This process optimizes the thermodynamical properties of the crystalline cyclic polylactides and is responsible for the high  $T_m$  and  $\Delta H_m$  values.

## 1. Introduction

Poly(L-lactide) (PLA) has become a widely used biodegradable material with the additional benefit to be synthesized from natural resources.<sup>[1–5]</sup> The technical production is based on alcohol-initiated ring-opening polymerizations (ROPs) catalyzed by tin(II) 2-ethyl hexanoate (SnOct<sub>2</sub>) and therefore, most preparative and mechanistic studies of ROPs of lactides were conducted with tin catalysts. Although SnOct<sub>2</sub> and other tin(II) salts have a low toxicity for humans, catalysts based on zinc might be an interesting alternative, because zinc ions belong to the human nutrition. ROP catalysts based on zinc have a long tradition in

the chemistry of PLAs beginning with the work of Kleine et al. in 1958.<sup>[6]</sup> In the following decades, zinc-based catalysts have been studied by numerous research groups.<sup>[7–34]</sup> Zinc powder and zinc oxide (which covers the surface of the zinc powder) were the first catalysts studied by several research groups. However, for medical or pharmaceutical applications the zinc powder needs to be removed from the PLA by filtration or centrifugation and ZnO showed a high tendency to racemize L-lactide. Therefore, the first author had focused his interest in the less basic zinc carboxylates, and it was found that with low concentration of zinc stearate or zinc caprylate no racemization occurs at 160 °C even at reaction times of several days.<sup>[16,35]</sup> The ROP


experiments with zinc carboxylates were conducted before 1998, at a time, when matrix-assisted laser desorption/ionization time of flight (MALDI-TOF) mass spectrometry was still in its infancy and not available in most laboratories.<sup>[15–21]</sup> Hence, information about formation of cyclic PLAs (cPLAs) and transesterification reactions in solution or in the melt was not available.

Over the past 15 years research on synthesis and characterization of cyclic polymers, in general,<sup>[36]</sup> and cPLA in particular<sup>[37–56]</sup> has found increasing interest. Cyclic polymers have a higher coil density than their linear counterparts with the consequence of lower melt and solution viscosities which may be advantageous for processing of high molar mass polymers from the melt. Furthermore, a higher thermal stability, slightly higher glass transition temperatures, and  $T_m$  values belong to the positive aspects of cyclic polymers.

cPLA can be prepared via two reaction mechanisms, either via ring expansion polymerization with cyclic catalysts or via a ring-opening polymerization with simultaneous polycondensation (ROPPOC) mechanism. For a review including a detailed definition and characterization of this new mechanism see ref. [57]. It is characteristic for the ROPPOC method that the initial ROP generates two reactive chain ends, so that simultaneously polycondensation and cyclization reactions may occur (Schemes 1 and 2). The ROPPOC approach may involve ionic chain ends, as it is typical for zwitterionic polymerizations<sup>[38–45]</sup> or covalent chain ends, as it is typical for tin(II) and tin(IV) compounds.<sup>[37,47,49,51]</sup>

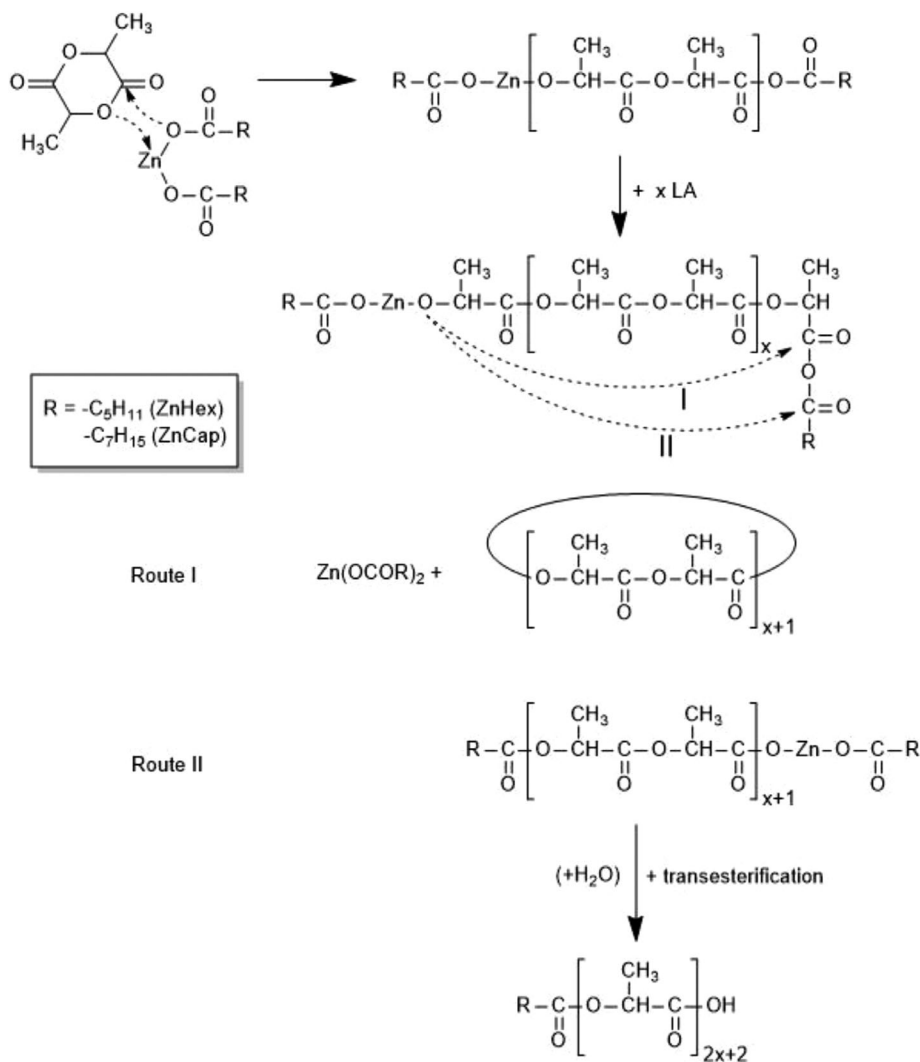
Quite recently the authors have shown that also zinc caprylate (ZnCap<sub>2</sub>) can catalyze the formation of cPLA via a ROPPOC method (Scheme 1).<sup>[35]</sup> However, the use of metal carboxylates

H. R. Kricheldorf, F. Scheliga  
 Institute for Technical and Macromolecular Chemistry  
 University of Hamburg  
 Bundesstr. 45, D 20146 Hamburg, Germany  
 E-mail: hrkricheldorf@aol.de; kricheld@chemie.uni-hamburg.de  
 S. M. Weidner  
 Federal Institute for Materials Research and Testing (BAM)  
 Richard Willstätter Str. 11, D-12489 Berlin, Germany

 The ORCID identification number(s) for the author(s) of this article can be found under <https://doi.org/10.1002/macp.202300070>

© 2023 The Authors. Macromolecular Chemistry and Physics published by Wiley-VCH GmbH. This is an open access article under the terms of the Creative Commons Attribution-NonCommercial-NoDerivs License, which permits use and distribution in any medium, provided the original work is properly cited, the use is non-commercial and no modifications or adaptations are made.

DOI: 10.1002/macp.202300070



**Scheme 1.** ZnHex (ZnCap) catalyzed ROPPOC mechanism.

has the disadvantage that formation of linear chains having COOH end groups may compete with formation of cPLA at least at low LA/Cat ratios. Furthermore, ZnCap<sub>2</sub> proved to be a rather sluggish catalyst with a polymerization activity ≈100 times lower than that of SnOct<sub>2</sub>. Hence, it was of interest to compare Zn carboxylates with Zn catalysts having Zn–S bonds such as ZnSPCl or ZnSPF (Scheme 2), because an alternative reaction pathway yielding linear chains does not exist. Furthermore, the reactivity of such Zn–S compounds was of interest because Zn–S based catalysts have never been used as catalysts for ROPs of lactide. Moreover, sulfides are less basic than the analogous oxides, so that the risk of racemization of L-lactide is lower. This aspect was important, because long annealing times (up to 7 d) were of interest. Another question which should be answered concerning the transesterification activity of the Zn–S catalysts (in comparison with Zn-hexanoate) in the modification of solid PLAs. In the case of tin-based catalysts,<sup>[52–54]</sup> it was found that modification of the surface of crystallites consisting of extended-cycles resulted in optimization of both  $T_m$  and  $\Delta H_m$ , and the progress of this optimization was also indicated by a so-called “saw tooth pattern”

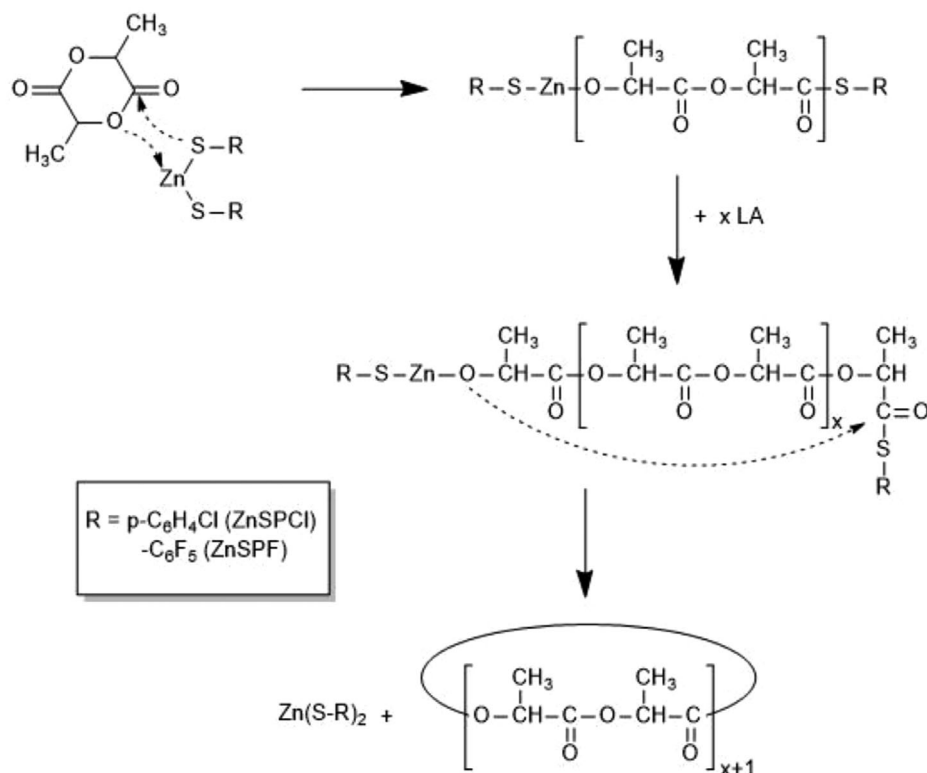
in the mass peak distribution in the MALDI mass spectra below  $m/z$  15 000.<sup>[55,56]</sup>

Finally, it should be mentioned that the synthesis of cyclic PLAs by means of a Zn catalyst ( $\text{ZnC}_6\text{F}_5$ )<sub>2</sub> was reported by Piedra-Arroni et al.<sup>[25]</sup> and Li et al.<sup>[26]</sup> Those authors performed their polymerizations in solution and obtained a low molar mass cyclic PLA with low dispersity. In contrast, the ZnS catalysts studied in this work were designed to allow for polymerization in bulk and to yield cPLA having  $M_w$  values above 100 000, with high dispersities, prerequisites for satisfactory processing from the melt and for good mechanical properties.

## 2. Experimental Section

### 2.1. Materials

L-Lactide, a product of Corbion-Purac, was kindly supplied by Thyssen-Uhde AG (Berlin) and recrystallized from “Toluene 99.99% extra dry” (ACROS Chemicals), diethyl zinc (1 M in *n*-hexane), *n*-hexanoic acid, 4-chlorothiophenol, and pentafluoroth-



**Scheme 2.** ZnSPF (ZnSPCl) catalyzed ROPPOC synthesis of cPLAs.

iphenol were purchased from Alfa Aesar (Kandel, Germany) and used as received. Anhydrous THF was purchased from Sigma-Aldrich.

### 2.1.1. Synthesis of Zinc *n*-Hexanoate (ZnHEX)

Diethyl zinc (20 mmol, 1 M in hexane) was added dropwise with stirring to a solution of *n*-hexanoic acid (40 mmol) in a mixture of THF (20 mL) and toluene (80 mL). The reaction mixture was concentrated in vacuo to  $\approx 50$  mL and ligroin 50 mL was added dropwise with stirring. After 20 h the white precipitate was isolated by filtration and dried in vacuo at 40 °C. Yield: 92%.  $T_m$ : 147 °C (DSC with a heating rate of 5 K min<sup>-1</sup>,  $T_m$  of ZCap = 137 °C). Elemental analyses: C calc. 48.2%, found 48.4%, H calc. 7.80%, found 7.48%. <sup>1</sup>H NMR: 2.08 (t, 4H), 1.46 (m, 4H), 1.25 (m, 8H), 0.86 (t, 6H) ppm.

### 2.1.2. Synthesis of Zinc 4-Chlorothiophenolate (ZnSPCl)

This catalyst was prepared analogously to ZHEX. Yield: 93%, no m.p., elemental analyses: C calc. 41.2%, found 40.5%, H calc. 2.27%, found 2.41%, S calc. 18.20%, found 17.7%, <sup>1</sup>H NMR: 7.29+7.27 (4H), 7.02+7.00 (4H) ppm.

### 2.1.3. Synthesis of Zinc Pentafluorothiophenolate (ZnSPF)

This catalyst was prepared analogously to ZHEX. Yield: 68%, no m.p., elemental analyses: C calc 30.5%, found, 31.1%; S calc. 13.80%, found 13.55%.

### 2.1.4. Polymerizations

**At 140 °C:** The catalyst (0.08 mmol) and L-lactide (40 mmol) were weighed into a flame-dried 50 mL Erlenmeyer flask under a blanket of argon and a magnetic bar was added. The reaction vessel was placed into an oil bath thermostated at 140 °C. After 1 d the reaction vessel was destroyed, and the crystalline plaque was cut or broken into six pieces. Two pieces were used for characterization, two pieces were annealed at 140 °C for three additional days in an atmosphere of argon and two pieces were annealed for additional 6 d in an atmosphere of argon.

**At 160 °C:** The catalyst (0.04 mmol) and L-lactide (40 mmol) were weighed into a flame-dried 50 mL Erlenmeyer flask under a blanket of argon and a magnetic bar was added. The reaction vessel was immersed into an oil bath thermostated at 160 °C. After 12 h part of the highly viscous melt was removed with a spatula or pincer and the remaining product was again thermostated at 160 °C for additional 12 h (Tables 1–3).

## 2.2. Measurements

All samples were characterized in the virgin state.

The 400 MHz <sup>1</sup>H NMR spectra were recorded with a Bruker Avance 400 FT NMR spectrometer in 5 mm sample tubes. DMSO-d<sub>6</sub> containing TMS served as solvent and shift reference.

The DSC measurements were conducted with a heating rate of 10 K min<sup>-1</sup> on a Mettler-Toledo DSC-1 equipped with Stare Software version 11.00. The sample size was in

**Table 1.** ROPPOCs catalyzed by ZnHEX in bulk with variation of LA/Cat ratio, temperature, and time.

Exp. no.	LA/Cat	Temp. [°C]	Time [d]	$M_n$	$M_w$	$T_m$ [°C]	$\Delta H_m$ [J g <sup>-1</sup> ]
1A	500/1	140	1	29 000	69 000	54.2	57.3
1B	500/1	140	4	49 000	108 000	189.3	87.2
1C	500/1	140	7	37 000	93 000	178.4	60.3
2A	1000/1	140	1	Low	convers.	–	–
2B	1000/1	140	4	1900	8500	131.7 + 166.6	40.2
3A	1000/1	160	0.5	31 000	93 000	Melt	–
3B	1000/1	160	1.0	28 000	73 000	163.1 <sup>b)</sup>	39.8

<sup>a)</sup> Conversion around 99% in all experiments <sup>b)</sup> Crystallization occurred after scratching of the surface of the molten PLA followed by annealing for 24 h.

**Table 2.** ROPPOCs catalyzed by ZnSPCL in bulk with variation of LA/Cat ratio, temperature, and time.

Exp. no.	LA/Cat	Temp. [°C]	Time [d]	$M_n$	$M_w$	$T_m$ [°C]	$\Delta H_m$ [J g <sup>-1</sup> ]
1A	500/1	140	1.0	39 000	120 000	Melt	–
1B	500/1	140	4.0	38 000	117 000	185.2	79.2
1C	500/1	140	7.0	36 000	110 500	192.3	94.5
2A	1000/1	160	0.5	19 500	47 500	Melt	–
2B	1000/1	160	1.0	33 000	89 500	187.8	77.1

<sup>a)</sup> Conversion around 97% for the molten samples and >99% for crystalline PLAs

the range of 8–11 mg. The system was rinsed with nitrogen at a flow rate of 50 mL min<sup>-1</sup>. Only the first heating was evaluated.

MALDI-TOF mass spectrometry was performed using an Autoflex max (Bruker Daltonik GmbH, Bremen) in the linear positive mode using *trans*-2-[3-(4-*tert*-butylphenyl)-2-methyl-2-propenylidene] malononitrile (DCTB) dissolved in chloroform (20 mg mL<sup>-1</sup>) as matrix. The solution was doped with potassium trifluoroacetate to enable selective potassium adduct ion formation. The matrix solution was premixed with the analyte solution (chloroform, 4 mg mL<sup>-1</sup>) in a ratio of 5/2 (v/v). 1  $\mu$ L of the resulting solution was deposited on the sample target. Typically, 8000 single spectra recorded at four different positions within one spot were accumulated. The instrument was previously calibrated with PEO standards.

For the GPC experiments a modular system kept at 40 °C (isocratic pump, 1 mL min<sup>-1</sup>, refractive index detector, Optilab reX, Wyatt) was applied. Samples dissolved in chloroform were manually injected (100  $\mu$ L, 2–4 mg mL<sup>-1</sup>). For instrument control and data calculation Astra 6.1 software (Wyatt Technology Europe GmbH, Dernbach) was used. The calibration was performed using polystyrene standard sets (Polymer Standards Service – PSS, Mainz, Germany).

## 3. Results and Discussion

### 3.1. Polymerizations Catalyzed by Zinc Hexanoate

ZnHEX was prepared by addition of a ZnEt<sub>2</sub> solution to a solution of n-hexanoic acid in toluene. The white crystalline precipi-

**Table 3.** ROPPOCs catalyzed by ZnSPF in bulk with variation of LA/Cat ratio, temperature, and time.

Exp. no. <sup>a)</sup>	LA/Cat	Temp. [°C]	Time [d]	$M_n$	$M_w$	$T_m$ [°C]	$\Delta H_m$ [J g <sup>-1</sup> ]
1A	500/1	140	0.5	54 000 52 500 <sup>b)</sup>	178 000 175 500 <sup>b)</sup>	–	–
1B	500/1	140	1	47 000	131 500	187.0	72.5
1C	500/1	140	4	40 000	106 000	196.3	91.3
1D	500/1	140	7	38 000	91 000	199.9	94.5
2A	1000/1	140	0.5	43 000	92 000	–	–
2B	1000/1	140	1	46 000	121 000	184.5	68.0
2C	1000/1	140	4	41 000	101 000	187.4	89.2
2D	1000/1	140	7	37 000	93 000	193.3	92.1
3A	1000/1	160	0.5	38 500	125 000	–	–
3B	1000/1	160	1.0	31 000	86 000	185.6	72.1

<sup>a)</sup> Conversion around 97% for molten samples and >99% for crystalline PLAs <sup>b)</sup> Repetition of the first measurement.

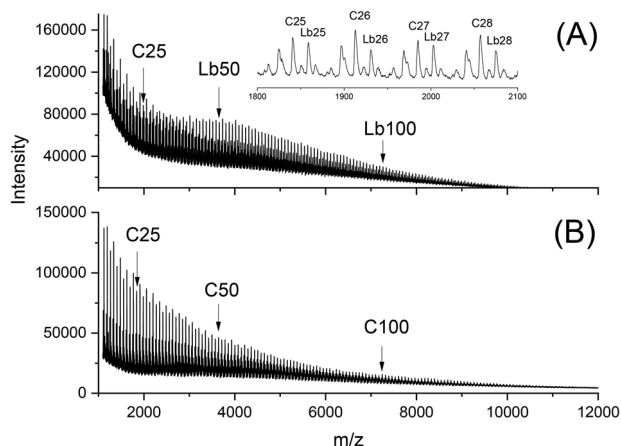


**Figure 1.** MALDI-TOF mass spectra of PLAs prepared with ZnHEX (LA/Cat = 500/1) at 140 °C: A) after 1 d (No. 1A, Table 1); B) after 7 d (No. 1C, Table 1).

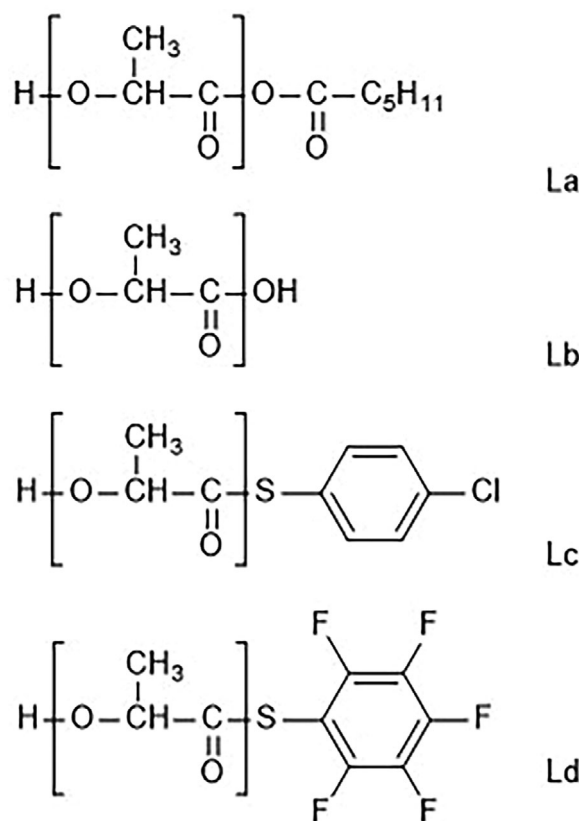
tate isolated from the reaction mixture was used without further purification (ZnSPCl and ZnSPF were prepared analogously). A first series of polymerizations was performed at 140 °C with variation of time (Table 1). With a LA/Cat ratio of 500/1 a polymerization time of 1 d did not suffice to reach the maximum molecular weight. The molecular weight passed a flat maximum at longer times and decreased after 4 d. The PLA isolated after 4 d was at least satisfactory in that a  $M_w$  slightly above 100 000 was achieved. Attempts to reach higher molecular weights with a LA/Cat ratio of 1000/1 failed. At 140 °C the polymerization was so slow that even after 4 d only a  $M_w < 10\,000$  was obtained (Nos. 2A, B). Analogous polymerizations at 160 °C were significantly faster, but a  $M_w > 100\,000$  was not achieved. These results confirmed the low reactivity of zinc carboxylates also observed for zinc caprylate in a previous publication.

The MALDI-TOF mass spectra of the samples Nos. 1A–1C revealed an increasing concentration of cyclic PLA (e.g.,  $25_{\text{mer}} = (72.06)_{\text{LA}} \times 25 + 39_{\text{K}} = 1840.7$ ; found 1840.8) with higher polymerization times as demonstrated by **Figure 1**. The predominant linear chains detectable in the mass spectrum of the 1d sample (No. 1A, Table 1) revealed a mass shift (compared to cyclics) of 18 Da, which is characteristic for the Lb chains outlined in **Scheme 3**.

They resulted from the hydrolysis of the Z–O bonds and of the anhydride end groups of the virgin PLA chains (Scheme 2). The longer polymerization times were in fact annealing times because the PLAs prepared under these conditions had crystallized after 1 d. Hence, these results indicate that transesterification reactions were still going on in the solid PLA, a conclusion confirmed by the change of  $T_m$  and  $\Delta H_m$ . A rather high  $T_m$  was observed after 4 d in connection with the maximum molecular weight, but a value above 190 °C was not achieved.

### 3.2. Polymerizations Catalyzed by Zinc 4-Chlorophenyl Sulfide

With ZnSPCl five polymerizations were performed under conditions analogous to those applied for the polymerizations with ZnHEX. The three experiments conducted at 140 °C (No. 1A–C, Table 2) revealed a higher catalytic activity than that of ZnHEX.

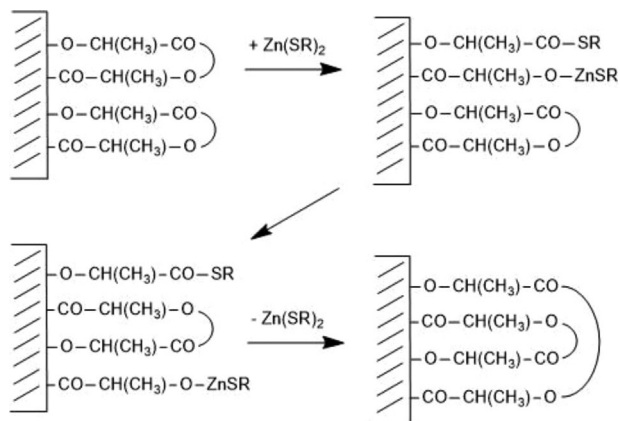


**Scheme 3.** Linear poly(lactides) discussed in this work and their labels used in Figures 1 and 6.

The maximum molecular weight was achieved at the shortest time and all molecular weights obtained at 140 °C were higher than those achieved with ZnHEX under identical conditions. The higher reactivity of the ZnSPCl catalyst was also evident from the higher  $T_m$  and higher  $\Delta H_m$  values obtained by the 140 °C experiments. This conclusion is based on the following consideration. The  $T_m$  of a polymer depends on various parameters including the surface free energy ( $\sigma_e$ ) according to the Gibbs–Thomson equation (1). From polymerization conducted with various tin catalysts it was learned that the presence of the catalyst in the solid PLA causes transesterification reactions (e.g., that of **Scheme 4**) which modify the surface of the crystallites in direction of a smoother surface with the consequence of a lower  $\sigma_e$ .<sup>[51–56]</sup> Furthermore, the thickness of the crystals increases at the expense of the amorphous phase and at the expense of the fraction of the immobile disordered phase on the surface. Both consequences of the transesterification reactions favor, in turn, higher  $T_m$ 's and higher crystallinities. Hence, the physical properties of crystalline PLA reflect the catalytic activity of the polymerization/transesterification catalysts when compared under identical conditions.

$$T_m = T_m^0 [1 - (2\sigma_e / \rho \Delta H_m^0 l_c)] \quad (1)$$

where  $T_m^0$  and  $\Delta H_m^0$  are the melting temperature and melting enthalpy of an ideal crystal, respectively;  $\rho$  is density of the crystal, and  $l_c$  is thickness of the lamellar crystal.



**Scheme 4.** 2D illustration of a rearrangement of neighboring loops via transesterification.

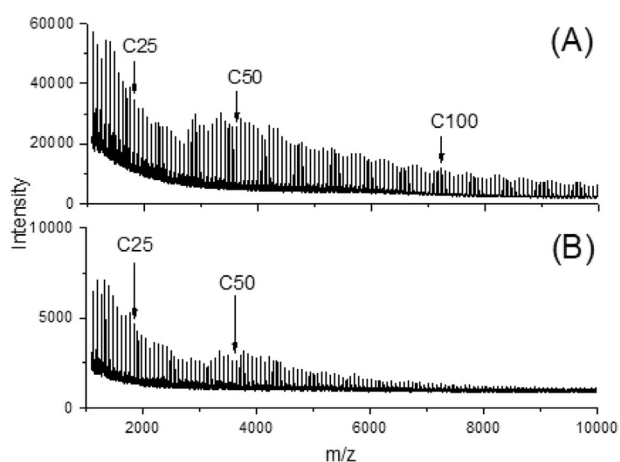


**Figure 2.** MALDI-TOF mass spectra of PLAs prepared with ZnSPCL (LA/Cat = 500/1) at 140 °C: A) after 4 d (No. 1B, Table 2); B) after 7 d (No. 1C, Table 2).

Concerning the MALDI-TOF mass spectrometry, the ZnSPCL is unfavorable because the molecular weight of chloro-thiophenol is almost identical with that of lactide (144 Da). Therefore, the mass spectra do not allow for a distinction between cyclic and linear PLAs bearing a chloro-thiophenolate end group (Lc in Scheme 3). Interestingly, the MALDI-TOF mass spectra of the PLAs isolated after annealing for 4 or 7 d at 140 °C displayed a so-called “saw tooth pattern” (Figure 2). Such “saw-tooth patterns” were found for numerous cyclic PLAs prepared under a variety of reaction conditions with tin(II) and tin(IV) catalysts,<sup>[52,53]</sup> but this pattern was never observed for crystalline linear PLAs. Hence, the “saw-tooth pattern” is an indirect but reliable indication for the formation of cyclic PLAs. The origin of the “saw-tooth pattern” has been discussed in several recent publications of the authors.<sup>[55,56]</sup> In the mass range of  $m/z$  3000–15 000 cyclic PLAs have the tendency to form extended-ring crystals, because these crystals represent the thermodynamically most perfect and stable type of crystalline PLA (Figure 3). First, the linear chain segments of cyclic PLAs are necessarily arranged in a perfect antiparallel 1:1 ratio, which is the thermodynamical optimum as known from the  $\alpha$ -modification.<sup>[58,59]</sup> Second, defects resulting from chain ends embedded in the crystal lattice are not present when the cycles

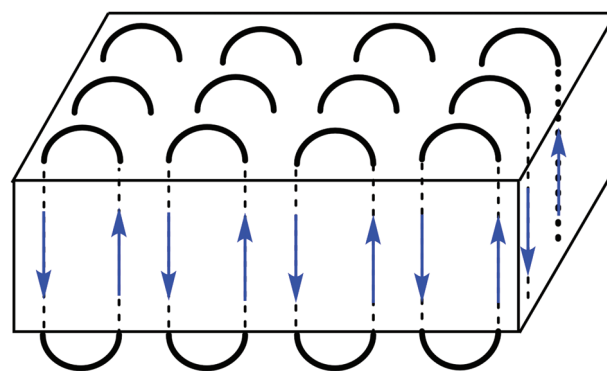


**Figure 3.** Schematic illustration of an extended-ring crystallite with smoothed surface.

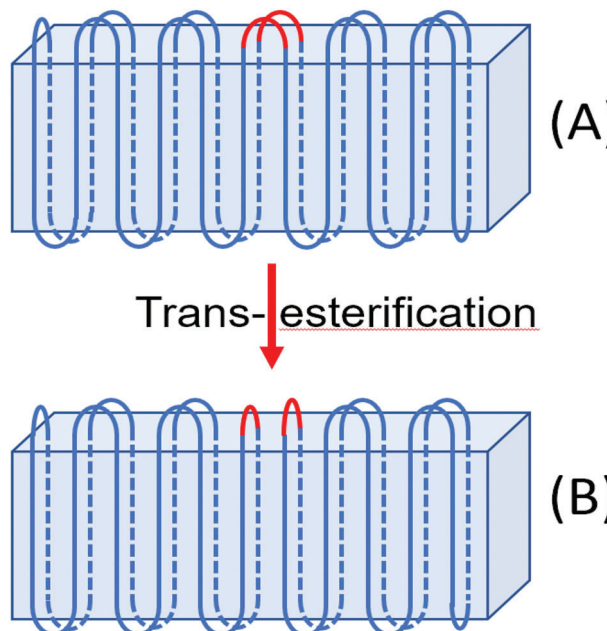


**Figure 4.** Transformation of two “fold loops” into two “end loops.”

have similar ring sizes. Third, when ring folding is absent, all loops on both surfaces are arranged in a parallel fashion. In the case of ring folding of long chains, the loops of folds take a perpendicular position relative to the loops of the (formal) ring ends (Figure 4). The “saw-tooth pattern” indicates a thermodynamical optimization of both surfaces of extended ring crystals. Each tooth represents a class of crystallites defined by identical ring size and ring size distribution. The maximum peak results from the most abundant ring size in these crystallites. It is mainly accompanied by cycles that differ by only one or two repeat units. The “saw-tooth patterns” observed for the PLAs prepared with ZnSPCL and ZnSPF are the first examples prepared with tin-free catalysts.

### 3.3. Polymerizations Catalyzed by Zinc Pentafluorophenyl Sulfide

The polymerizations catalyzed with ZnSPF were conducted quite analogously to those performed with the other zinc catalysts (Table 3). Several results allow for the conclusion that ZnSPF is

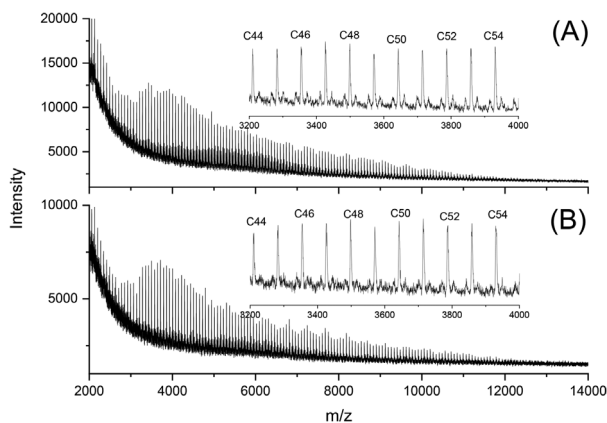


**Figure 5.** MALDI-TOF mass spectra of PLAs prepared with ZnSPF (LA/Cat = 500/1) at 140 °C: A) after 1 d (No. 1, Table 3); B) after 7 d (No. 3, Table 3).

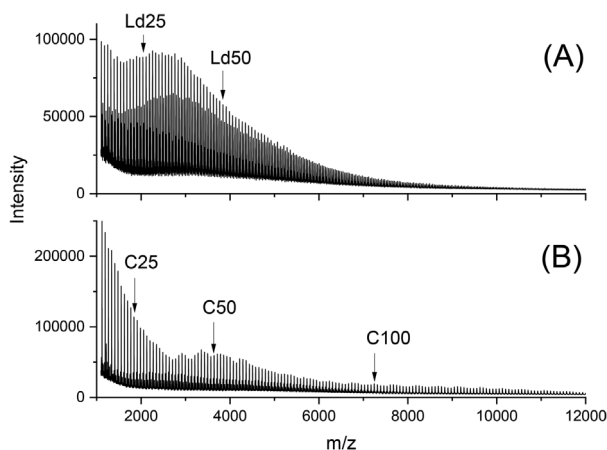


**Figure 6.** MALDI-TOF mass spectra of PLAs prepared with ZnSPF (LA/Cat = 1000/1) at 140 °C: A) after 1 d (No. 4, Table 3); B) after 7 d (No. 7, Table 3).

the most effective catalyst used in the present work. First, the highest molecular weights were obtained with  $M_w$  values above 120 000. The highest value was achieved by polymerization in bulk at the shortest reaction time (No. 1, Table 3). Second, ZnSCF also catalyzes a conspicuous degradation of the molecular weight upon annealing at 140 °C (Nos. 1–4, Table 3) which proceeds even in the solid state (s. discussion below). Third, the highest  $T_m$ , close to the maximum of 201 °C reported for Sn-catalyst was achieved with ZnSPF (No. 1D, Table 3). Fourth, the highest crystallinity was found indicating efficient smoothing of the surface of the crystallites. In agreement with this interpretation a “saw-tooth pattern” became detectable after annealing for 4 d (Figure 5).

When the polymerizations conducted at 140 °C with a LA/Cat ratio of 500/1 were repeated with a LA/Cat ratio of 1 000/1 an interesting new phenomenon was observed. When the PLA was isolated after 0.5 or 1 d the mass peaks of linear chains having a pentafluoro thiophenolate ester end group (Ld in Scheme 3) were the predominant species (Figure 6A). These mass peaks vanished upon further heating, and after 7 d the mass spectrum almost exclusively displayed the mass peaks of cycles (Figure 6B). The mass spectrum of the “7 d sample” also displayed a weak saw tooth pattern.”

These observations allow for two interesting conclusions. First, the detection of the Ld chains at relatively short polymerization times clearly proves the ROPPOC mechanism outlined in Scheme 2. Second, the finding that formation of the “saw-tooth pattern” requires 7 d and is not well developed when compared with the mass spectrum of Figure 5B, demonstrates that its appearance depends on the concentration of the catalyst. This finding is, in turn, consistent with the above interpretation that the formation of the “saw-tooth pattern” is a consequence of transesterification reactions and not of physical phenomena such as reptation of chains or cycles. The rather rapid degradation observed for the 140 °C experiments with a LA/Cat ratio of 500/1 also fits in with this interpretation. Considering the high crystallinity of the PLAs annealed for 4 or 7 d, it is unlikely that the degradation exclusively depends on ring-ring equilibration of the amorphous phase with formation of smaller cycles.

The largest fraction of the noncrystalline phase is certainly the immobile disordered phase, which covers the surface of the crystallites, so that the true amorphous fraction amounts to only a few percent. Degradation via ring-ring equilibration may indeed happen, but a complementary process which involves the crystallites is illustrated in Figure 4 and in Scheme 4. As previously discussed,<sup>[52]</sup> cyclic PLAs having masses > 15 000 Da must fold, to fit into lamellar crystallites having a thickness in the range of 16–26 nm as they are typical for annealed cyclic PLAs.<sup>[49–51]</sup> Hence, the presence of loops resulting from folding of large cycles is quite normal in PLAs having  $M_n$ 's > 15 000. When the parallel loops of folded PLAs undergo transesterification, so that perpendicular loops of “ring end groups” are formed, the molecular weight of a large cycle will be halved. Hence, only rather few such loop transformations are needed to cause a significant degradation of the molecular weight and the stability or perfection of the crystal lattice is not affected.

Finally, it should be mentioned that the higher effectiveness of ZSPF as transesterification catalysts relative to ZSPCl parallels the higher reactivity of  $Bu_2Sn(S-C_6F_5)_2$  as polymerization and cyclization catalyst relative to  $Bu_2Sn(S-C_6H_4Cl)_2$  reported in a previous publication.<sup>[60]</sup> When the Zn-SR or the Sn-SR group opens an ester group (first line in Scheme 2), the resulting CO-S-C<sub>6</sub>F<sub>4</sub> group is more electrophilic than the CO-S-C<sub>6</sub>H<sub>4</sub>Cl group due to the electron-withdrawing effect of the F-atoms, whereas the metal-O-CH group is the same. Apparently, the reactivity of the CO-SR group plays a key role for the catalytic activity of these metal sulfide catalysts.

### 3.4. About the Influence of (Non)Solvents

In a previous publication dealing with ring expansion polymerization of lactide by means of a cyclic tin catalyst, it was found that addition of small amounts (e.g., 4 vol%) of a so-called (non)solvent improves the mobility and thus, the transesterification efficiency in the solid PLA. (Non)solvent means in this context that the added liquid is a solvent for the monomer and low oligomers but a nonsolvent for crystalline PLA. High  $T_m$ 's (up to 201 °C) and high crystallinities ( $\Delta H_m$  up to 106 J g<sup>-1</sup>, corresponding to crystallinities up to ≈92%) were found.<sup>[61]</sup> Furthermore, the mass spectra of the annealed cyclic PLAs displayed the saw-tooth pattern characteristic for cyclic PLAs forming extended-

**Table 4.** ROPs catalyzed by ZnSPF (LA/Cat = 500/1) with addition of a nonsolvent ( $\approx 4$  vol%).

Exp. no.	Nonsolvent	Time [d]	$M_n$	$M_w$	$T_m$ [°C]	$\Delta H_m$ [J g <sup>-1</sup> ]
1A	<i>o</i> -Xylol	1	40 000	106 000	184.3	64.5
1B	<i>o</i> -Xylol	4	27 000	70 000	187.9	87.6
1C	<i>o</i> -Xylol	7	25 000	60 000	189.5	92.4
2A	Chlorobenzene	1	37 500	98 000	177.4	61.2
2B	Chlorobenzene	4	39 000	70 000	188.5	83.7
2C	Chlorobenzene	7	26 000	66 000	190.6	91.7
3A	Anisol	1	63 000	146 000	176.8	48.3
3B	Anisol	4	36 000	90 000	191.3	83.7
3C	Anisol	7	32 000	76 000	192.4	92.3

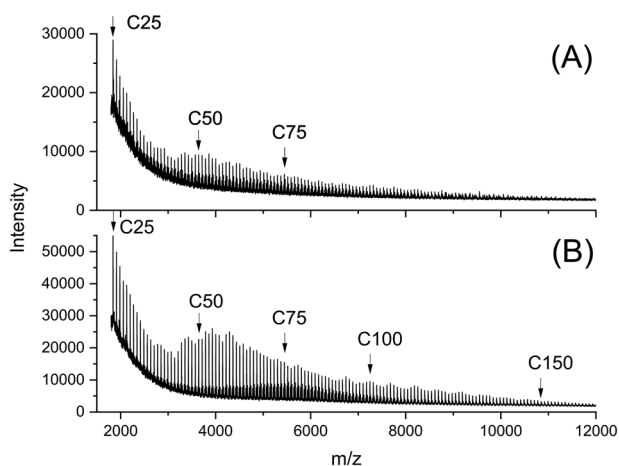


**Figure 7.** MALDI-TOF mass spectra of PLAs prepared with ZnSPF (LA/Cat = 500/1) at 140 °C: A) after 4 d with addition of chlorobenzene (No. 2B, Table 4); B) after 4 d with addition of anisole (No. 3B, Table 4).

ring crystals in the mass range of  $m/z$  3000–15 000. However, the influence of the (non)solvent depended very much on its nature, and the best results were obtained with anisole followed by chlorobenzene. Considering these previous results, anisole, chlorobenzene, and 1,2-xylene were selected for the present study, in as much as these three solvents were commercially available in anhydrous quality and with an extraordinary high level of purity. The results of the polymerizations performed at 140 °C were summarized in Table 4.

When the molecular weights, the  $T_m$  and  $\Delta H_m$  values are taken as measure of the quality of the (non)solvents, the following order of increasing effectiveness was found in agreement with the previous work of cyclic tin catalysts; 1,2-xylene < chlorobenzene < anisole. This order was confirmed by the shape of the MALDI-TOF mass spectra. The “saw-tooth pattern” characteristic for optimized extended-ring crystals was not observed for the PLAs prepared with addition of 1,2-xylene. It was detectable in the mass spectra of the samples prepared with addition of chlorobenzene (Figure 7A), and it was more pronounced in the mass spectrum of the anisole-containing PLA as illustrated by Figure 7B. These findings allow for two conclusions. First, addition of a small amount of a (non) solvent has an influence on the efficiency of transesterification reaction on the surface of the

crystallites. Second, the positive influence decreases in the order: *o*-xylene < chlorobenzene < anisole. The same trend was found for annealing of cyclic PLAs with cyclic tin catalysts. From unpublished polymerization experiments the authors have learned that the solubility of PLAs also increases in this order, because increasing polarity of these relatively low polar solvents favors the solvation of PLA. Hence, it may be assumed that improved solvation of PLA loops and chain segments supports their transesterification. (Supporting information)

## 4. Conclusions

Three conclusions may be drawn from the results of this work. First, the reactivity of the three catalysts increases in the order: ZnHeEX < ZnSPCl < ZnSPF. Second, with ZnSPF  $M_w$  values above 170 000 can be achieved within 12 h at 140 °C. Third, the relatively high reactivity of ZnSPF enables transesterification reactions (mainly ring-ring equilibration) in the solid PLAs which entail a thermodynamical optimization of the crystallites. Characteristic consequences of this optimization are  $T_m$  values up to 199 °C, and  $\Delta H_m$  values up to 99 J g<sup>-1</sup>, close to the maxima reported to cyclic PLAs prepared and annealed with cyclic tin catalysts.

## Supporting Information

Supporting Information is available from the Wiley Online Library or from the author.

## Acknowledgements

The authors wish to thank Ing. A. Myxa (BAM, Berlin) for the GPC measurements and S. Bleck (TMC, Hamburg) for the DSC measurements. The authors also thank Dr. Simon Rost (Elantas/Altana AG, Hamburg) for financial support.

Open access funding enabled and organized by Projekt DEAL.

## Conflict of Interest

The authors declare no conflict of interest.

## Data Availability Statement

The data that support the findings of this study are available from the corresponding author upon reasonable request.



## Keywords

cyclization, lactide, MALDI-TOF MS, ring-opening polymerization, zinc salts

Received: March 13, 2023

Revised: May 22, 2023

Published online:

- [1] I. Armentano, N. Bitinis, E. Fortunati, S. Mattioli, N. Rescignano, R. Verdejo, M. A. Lopez-Manchado, J. M. Kenny, *Prog. Polym. Sci.* **2013**, 38, 1720.
- [2] R. A. Auras, L.-T. Lim, S. E. Selke, H. Tsuji, *Poly (Lactic Acid): Synthesis, Structures, Properties, Processing, and Applications*, John Wiley & Sons, New York **2011**.
- [3] M. L. Di Lorenzo, R. Androsch, in *Synthesis, Structure and Properties of Poly(lactic acid)* (Eds: M. L. Di Lorenzo, R. Androsch, *Advances in Polymer Science*, Springer, Cham **2017**, 279.
- [4] M. L. Di Lorenzo, R. Androsch, in *Industrial Applications of Poly(lactic acid)* (Eds: M. L. Di Lorenzo, R. Androsch, *Advances in Polymer Science*, Springer, Cham **2018**, 282.
- [5] R. P. Pawar, S. U. Tekale, S. U. Shisodia, J. T. Totre, A. J. Domb, *Recent Patents Regener. Med.* **2014**, 4, 40.
- [6] V. J. Kleine, H.-H. Kleine, *Macromol. Chem. Phys.* **1959**, 30, 23.
- [7] T. Tsuruta, K. Matsuura, S. Inoue, *Macromol. Chem. Phys.* **1964**, 75, 211.
- [8] V. W. Dittrich, R. C. Schulz, *Macromol. Chem. Phys.* **1971**, 15, 109.
- [9] E. Lillie, R. C. Schulz, *Macromol. Chem. Phys.* **1975**, 176, 1901.
- [10] M. Vert, F. Chabot, J. Leray, P. Christel, *Makromol. Chem. Suppl.* **1981**, 5, 30.
- [11] F. Chabot, M. Vert, S. Chapelle, P. Granger, *Polymer* **1983**, 24, 53.
- [12] G. Schwach, J. Coudane, R. Engel, M. Vert, *Polym. Bull.* **1994**, 32, 617.
- [13] J. Coudane, C. Ustariz-Peyret, G. Schwach, M. Vert, *J. Polym. Sci., Part A: Polym. Chem.* **1997**, 35, 1651.
- [14] G. Schwach, J. Coudane, R. Engel, M. Vert, *Polym. Int.* **1998**, 46, 177.
- [15] H. R. Kricheldorf, C. Boettcher, *J. Macromol. Sci., Part A: Pure Appl. Chem.* **1993**, A30, 441.
- [16] H. Kricheldorf, A. Serra, *Polym. Bull.* **1985**, 14, 497.
- [17] M. Bero, J. Kasperczyk, Z. J. Jedlinski, *Macromol. Chem. Phys.* **1990**, 191, 2287.
- [18] H. R. Kricheldorf, D.-O. Damrau, *Macromol. Chem. Phys.* **1998**, 199, 1089.
- [19] H. R. Kricheldorf, D.-O. Damrau, *Macromol. Chem. Phys.* **1997**, 198, 1753.
- [20] H. R. Kricheldorf, D.-O. Damrau, *Macromol. Chem. Phys.* **1998**, 199, 1747.
- [21] I. Kreiser-Saunders, H. R. Kricheldorf, *Macromol. Chem. Phys.* **1998**, 199, 1081.
- [22] D. Zhang, J. Xu, L. Alcazar-Roman, L. Greenman, C. J. Cramer, M. A. Hillmyer, W. B. Tolman, *Macromolecules* **2004**, 37, 5274.
- [23] M. F. Pastor, T. J. J. Whitehorne, P. O. Oguadinma, F. Schaper, *Inorg. Chem. Commun.* **2011**, 14, 1737.
- [24] S. Nayab, H. Lee, J. H. Jeong, *Polyhedron* **2012**, 43, 55.
- [25] E. Piedra-Arrión, C. Ladavière, A. Amgoune, D. Bourissou, *J. Am. Chem. Soc.* **2013**, 135, 13306.
- [26] X.-Q. Li, B. Wang, H.-Y. Ji, Y.-S. Li, *Catal. Sci. Technol.* **2016**, 6, 7763.
- [27] Z. Luo, S. Chaemchuen, K. Zhou, A. A. Gonzalez, F. Verpoort, *Appl. Catal., A* **2017**, 546, 15.
- [28] P. P. Rade, B. Garnaik, *Int. J. Polym. Anal. Charact.* **2020**, 25, 283.
- [29] F. Chotard, R. Lapenta, A. Bolley, A. Trommenschlager, C. Balan, J. Bayardon, R. Malacea-Kabbara, Q. Bonnin, E. Bodio, H. Cattey, P. Richard, S. Milione, A. Grassi, S. Dagorne, P. Le Gendre, *Organometallics* **2019**, 38, 4147.
- [30] P. M. Schäfer, K. Dankhoff, M. Rothemund, A. N. Ksiazkiewicz, A. Pich, R. Schobert, B. Weber, S. Herres-Pawlis, *ChemistryOpen* **2019**, 8, 1020.
- [31] P. M. Schäfer, S. Herres-Pawlis, *ChemPlusChem* **2020**, 85, 1044.
- [32] J. Stewart, M. Fuchs, J. Payne, O. Driscoll, G. Kociok-Köhn, B. D. Ward, S. Herres-Pawlis, M. D. Jones, *RSC Adv.* **2022**, 12, 1416.
- [33] M. Fuchs, M. Walbeck, E. Jagla, A. Hoffmann, S. Herres-Pawlis, *ChemPlusChem* **2022**, 87, 202200029.
- [34] N. Conen, M. Fuchs, A. Hoffmann, S. Herres-Pawlis, A. Jupke, *Adv. Sustainable Syst.* **2023**, 7, 2200359.
- [35] H. R. Kricheldorf, S. M. Weidner, F. Scheliga, *J. Polym. Sci., Part A: Polym. Chem.* **2022**, 60, 3222.
- [36] H. R. Kricheldorf, *J. Polym. Sci., Part A: Polym. Chem.* **2010**, 48, 251.
- [37] H. R. Kricheldorf, N. Lomadze, G. Schwarz, *Macromolecules* **2008**, 41, 7812.
- [38] W. Jeong, J. L. Hedrick, R. M. Waymouth, *J. Am. Chem. Soc.* **2007**, 129, 8414.
- [39] E. J. Shin, W. Jeong, H. A. Brown, B. J. Koo, J. L. Hedrick, R. M. Waymouth, *Macromolecules* **2011**, 44, 2773.
- [40] H. A. Brown, S. Xiong, G. A. Medvedev, Y. A. Chang, M. M. Abu-Omar, J. M. Caruthers, R. M. Waymouth, *Macromolecules* **2014**, 47, 2955.
- [41] E. J. Shin, H. A. Brown, S. Gonzalez, W. Jeong, J. L. Hedrick, R. M. Waymouth, *Angew. Chem., Int. Ed.* **2011**, 50, 6388.
- [42] G. Si, S. Zhang, W. Pang, F. Wang, C. Tan, *Polymer* **2018**, 154, 148.
- [43] A. V. Prasad, L. P. Stubbs, Z. Ma, Z. Yinghui, *J. Appl. Polym. Sci.* **2012**, 123, 1568.
- [44] Y. A. Chang, A. E. Rudenko, R. M. Waymouth, *ACS Macro Lett.* **2016**, 5, 1162.
- [45] S. Praban, S. Yimthachote, J. Kiriratnikom, S. Chotchatchawankul, J. Tantirungrotechai, K. Phomphrai, *J. Polym. Sci., Part A: Polym. Chem.* **2019**, 57, 2104.
- [46] H. R. Kricheldorf, S. M. Weidner, F. Scheliga, *Macromol. Chem. Phys.* **2017**, 218, 1700274.
- [47] H. R. Kricheldorf, S. M. Weidner, F. Scheliga, *J. Polym. Sci., Part A: Polym. Chem.* **2017**, 55, 3767.
- [48] H. R. Kricheldorf, S. M. Weidner, F. Scheliga, *Polym. Chem.* **2017**, 8, 1589.
- [49] H. R. Kricheldorf, S. M. Weidner, *Eur. Polym. J.* **2018**, 109, 360.
- [50] H. R. Kricheldorf, S. M. Weidner, F. Scheliga, *J. Polym. Sci., Part A: Polym. Chem.* **2019**, 57, 952.
- [51] H. R. Kricheldorf, S. M. Weidner, *Polym. Chem.* **2020**, 11, 5249.
- [52] H. R. Kricheldorf, S. M. Weidner, A. Meyer, *Polym. Chem.* **2020**, 11, 2182.
- [53] S. M. Weidner, A. Meyer, S. Chatti, H. R. Kricheldorf, *RSC Adv.* **2021**, 11, 2872.
- [54] A. Meyer, S. M. Weidner, H. R. Kricheldorf, *Polymer* **2021**, 231, 124122.
- [55] S. M. Weidner, A. Meyer, H. R. Kricheldorf, *Polymer* **2022**, 255, 125142.
- [56] H. R. Kricheldorf, S. M. Weidner, A. Meyer, *Polymer* **2022**, 263, 125516.
- [57] H. R. Kricheldorf, S. M. Weidner, *Macromol. Rapid Commun.* **2020**, 41, 2000152.
- [58] P. De Santis, A. J. Kovacs, *Biopolymers* **1968**, 6, 299.
- [59] B. Lotz, in *Crystal Polymorphism and Morphology of Poly(lactides)*, *Advances in Polymer Sciences*, vol. 279, Springer, Cham **2018**, p. 273.
- [60] H. R. Kricheldorf, S. M. Weidner, A. Meyer, *Macromol. Chem. Phys.* **2022**, 224, 2200385.
- [61] H. R. Kricheldorf, S. M. Weidner, F. Scheliga, *J. Polym. Sci., Part A: Polym. Chem.* **2017**, 55, 3767.